ASSESSMENT OF THE SPATIAL VARIABILITY OF CWSI WITHIN ALMOND TREE CROWNS AND ITS EFFECTS ON THE RELATIONSHIP WITH STOMATAL CONDUCTANCE

Carlos Camino, Pablo J. Zarco-Tejada and Victoria González-Dugo

Instituto de Agricultura Sostenible (IAS), Consejo Superior de Investigaciones Científicas (CSIC), Alameda del Obispo s/n, 14004 Córdoba, Spain

ABSTRACT

This work focuses on understanding the effects caused by the within-tree structural heterogeneity on the Crop Water Stress Index (CWSI). We present an assessment of the CWSI variability and its relationship with stomatal conductance (Gs) using different automatic object-based tree-crown detection algorithms based on temperature quartile thresholds. The study was carried out in an almond orchard cultivated under three irrigated regimes. High-resolution (25 cm) thermal imagery was acquired by an aircraft on summer 2015. The tree crowns were segmented into 4 classes using the 25th, 50th and 75th percentiles via automatic object-based methods. Results showed that CWSI was linearly and inversely correlated with Gs in all thermal classes. However, the relationship with Gs was heavily affected by the crown segmentation levels applied, and improved remarkably when CWSI values where those corresponding to the coldest and purest vegetation pixels (r^2 =0.78 from pure vegetation pixels vs. r^2=0.52 when warmer pixels were used).

Index Terms— CWSI, Thermal imagery, stomatal conductance, tree-crown segmentation.

1. INTRODUCTION

The Crop Water Stress Index (CWSI) [1], [2]) is the most common indicator of water stress derived from thermal imagery, which is inversely related to transpiration and stomatal conductance [2], [3]. CWSI is based on the difference between canopy temperature and air temperature (Tc-Ta), normalized by the vapor pressure deficit (VPD). Water stress induces stomatal closure, thereby decreasing evaporative cooling and increasing leaf temperature [1], [4], [5]. In this regard, the CWSI, is an usefully tool for detecting water stress as demonstrated in several studies initiated in the late 1970s [2], [3]. Most of the field measurements that are currently used to characterize tree water relations are carried out at the leaf level, such as leaf water potential and stomatal conductance. However, these leaf measurements require a large number of field observations to adequately characterize the spatial patterns of water stress across an entire orchard. In this regard, remote sensing using stress indicators derived from thermal aerial imagery have been widely used to accurately describe the spatial heterogeneity of water stress on entire fields. In fact, several studies have shown that high-resolution thermal imagery acquired from manned [6] and unmanned aerial platforms [3],[7], [8] enabled the detection of water stress, yielding errors less than 1 K in the estimation of surface temperature of pure vegetation. Thermal imaging reveals spatial heterogeneity within and between plant canopies, and it can be acquired to monitor stress conditions over time [7], [9],[10].

The goal of this study was to determine which areas of tree crowns using high-resolution thermal images acquired from an aerial platform are more suitable for detecting water stress. In addition, we assess the way they influence the relationships with field-measured stomatal conductance.

2. MATERIAL AND METHODS

2.1. Study site

An experiment was carried out on July and August 2015 in an almond orchard comprising regulated deficit irrigation (RDI) treatments and rainfed conditions (RC). The site was located in Córdoba, Southern Spain at Alameda del Obispo Research Station (37″52'N, 4″49'W). In this work, three watering regimes were compared. A rainfed plot was compared with two irrigated treatments; a control treatment (T1) and severe RDI (T3). The irrigated treatments were replicated 4 times using a randomize block design (Fig. 1). Field measurements of stomatal conductance (Gs; $mmol·m^{-2}·s^{-1}$) were collected on four leaves per tree with a leaf porometer (SC-1, Decagon Devices Inc., Pullman, WA, USA).

2.2. Airborne campaigns

Three airborne campaigns were performed in 2015 on the day of the year (DOY) 182, 217, and 237 using a thermal infrared camera (FLIR SC655, FLIR Systems, Wilsonville, OR, USA) on board a Cessna aircraft operated by the Laboratory for Research Methods in Quantitative Remote Sensing (QuantaLab), Consejo Superior de Investigaciones

Científicas (IAS-CSIC, Spain). The thermal camera used in this study acquired imagery at a resolution of 640 × 480 pixels with a 13.1 mm focal length lense, providing an angular FOV of 45° x 33.7°, yielding a ground resolution of 25 cm. After each flight, the thermal images were processed in the laboratory as described by [9].
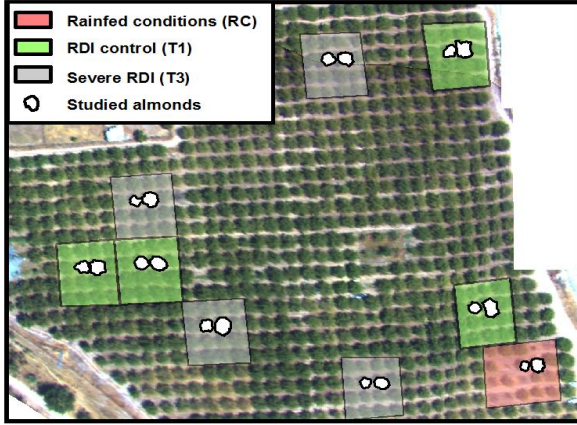
Fig. 1. Overview of the entire almond orchard site acquired by the hyperspectral sensor, showing the four replicates of the RDI treatments and the rainfed-condition block.

2.3. Segmentation and classification schemes

The individual tree crowns identified on the high-resolution thermal imagery were segmented based on quartile breaks. The image segmentations were automatically conducted using R software [11]. First, an object-based tree crown detection algorithm based on watershed segmentation (thresholds) was applied to separate the almond crown from the soil background ((Fig. 2a). Second, each tree crown was divided into four quartiles for extracting the mean canopy temperature from each quartile. The pixels of individual tree crowns were divided into 4 classes using the 25th, 50th and 75th percentiles (Fig. 2b). The proposed four quartile classes were as follows: i) first lower quartile (Q_{25}) associated with the coldest and purest vegetation areas without soil background, ii) quartile between Q_{25} and the middle quartile (Q_{50}), iii) quartile between Q_{50} and upper quartile (Q_{75}) and iv) the upper quartile (Q_{75}) associated with the warmest areas mainly affected by soil background.

3. RESULTS

3.1. CWSI heterogeneity as a function of within tree-crown segmentations

The crown temperature segmentations performed by automatic quartile detection from the high-resolution thermal imagery showed that the soil background effects were higher in pixels included into the quartile Q_{50}-Q_{75} and Q_{75} than in Q_{25} and Q_{25}-Q_{50}. This is explained by the high variability of CWSI present in the Q_{75} and Q_{50}-Q_{75}

segmentations (Table I). This within tree-crown variability was modulated by the large heterogeneity of vegetation and background pixels. Pixels contained in crown areas below the 50th percentile (Q_{25} and Q_{25}-Q_{50}) corresponded to pure vegetation pixels without soil contamination (Fig. 2b).
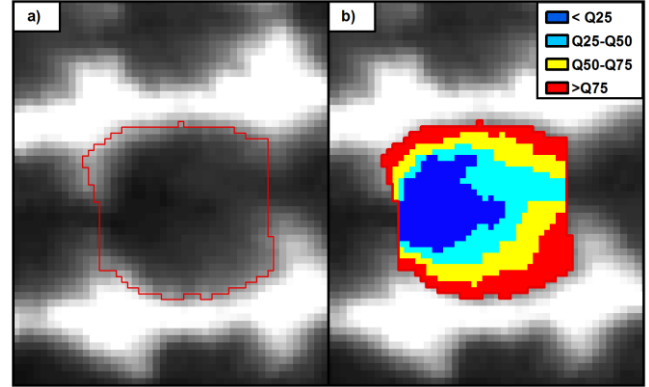
Fig. 2. View of a complete crown within the thermal imagery (a) and the quartile classes obtained using the quartile segmentation method (b).

Table I. Mean CWSI and standard deviation for each water stress treatments as a function of quartile levels.

	<Q_{25}	Q_{25}-Q_{50}	Q_{50}-Q_{75}	>Q_{75}	<Q_{50}
RC	0.97/0.24	1.22/0.21	1.55/0.17	1.98/0.16	1.05/0.22
T3	0.20/0.26	0.39/0.26	0.70/0.26	1.31/0.26	0.29/0.26
T1	-0.09/0.13	0.08/0.12	0.30/0.14	0.88/0.20	0.01/0.12

In almond trees, rainfed treatment resulted in small crowns, low leaf density and stomatal closure, caused by the long-term water stress imposed in this experiment. As a consequence, even for Q_{25}, values were close to the theoretical highest CWSI value of one. The CWSI values registered for RC were strongly affected by soil background. Nevertheless, and according to Gs values, leaf temperature agreed with values close to unity. The quartile crown segmentations also showed that CWSI values were biased on the Q_{50}-Q_{75} and upper quartile (Q_{75}) for all watering regimes, as consequence of soil background effects. As a result, the mean CWSI values were moved towards upper out-of-range values. In general, the CWSI values retrieved from the lower quartile (50th percentile) were within the theoretical CWSI range for the irrigated regimes. However, the mean CWSI value registered on RC treatment for Q_{25}-Q_{50} was slightly upper the maximum theoretical CWSI value. This bias was solved aggregating pixels of the two classes below the 50th percentile, yielding a mean CWSI of 1.05 for almond trees placed in RC. Similar correction is observed in the almond trees placed in irrigated regimes.

3.2. Relationships between crown segmentation CWSI levels and stomatal conductance

The average CWSI quantified from each tree-crown of the experiment were compared with the mean stomatal conductance across all dates for all segmentations based on the quartile thresholds. As expected, Fig. 3 shows that the mean CWSI was linearly and inversely correlated with stomatal conductance in all quartile classes. However, the relationships showed a large variability in CWSI depending on the quartile-crown segmentations conducted. In this regard, the CWSI values extracted from the upper quartile (Q_{75}) shifted towards high values of CWSI probably caused by the soil background effects, while for median quartile (Q_{50}) and complete crown pixels the CWSI values were lower than 1 for irrigated regimes. The relationships with Gs improved remarkably when the CWSI values corresponded to the coldest and purest vegetation areas associated to middle quartile-crown segmentations (Q_{50}), yielding $r^2=0.78$. However, the agreement with field-measured stomatal conductance yielded a weaker coefficient of determination for Q_{75} ($r^2 <0.52$, p-value < 0.005).
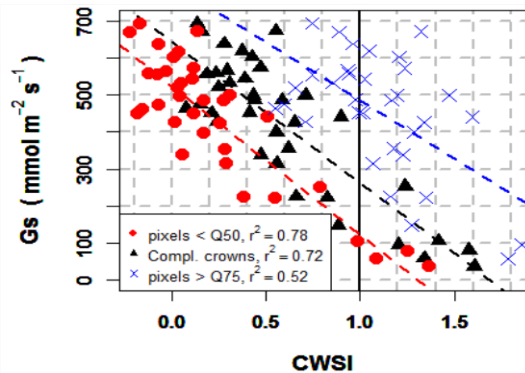
Fig. 3. Relationships obtained between leaf stomatal conductance (Gs) and CWSI extracted from complete crowns, median quartile pixels (Q_{50}) and the upper quartile pixels (Q_{75}) for all flight dates.

4. DISCUSSION

The methodology based on temperature quartile for crown segmentation using high-resolution thermal imagery demonstrated the value of the thermal-based index CWSI for monitoring transpiration processes, thus offers an alternative to conventional methods of irrigation performance assessment. In this study, we analyzed the CWSI variability over the different crown areas and its relation with stomatal conductance measured at leaf level. The quartile segmentation methods enabled the characterization of the temperature distribution from pure vegetation within individual tree crowns reducing the soil background effects. This study shows that crown CWSI extracted from upper quartile-crown segmentations (Q_{75}), highly affected by soil pixels (Fig. 3), yielded weaker (although still significant) relationship with stomatal conductance ($r^2 =0.52$ and p-value <0.005), compared to CWSI extracted from pure vegetation areas associated to

lower quartile-crown segmentations ($r^2 =0.78$ and p-value <0.005). The good agreement with stomatal conductance confirms the use of CWSI as a stress indicator in precision agriculture applications. In agreement with recent studies [8], [12], this study also showed that the CWSI is a reliable tool for monitoring the spatial variability of water stress using high-resolution thermal imagery.

5. CONCLUSION

This study highlights the need for high-resolution (25 cm or better) thermal imagery to adequately calculate CWSI values in orchard tree crowns. The work demonstrated the ability to track stress levels in almond crops using thermal imagery under different water stress conditions. It also demonstrates that canopy architecture, including shaded areas and soil background, needs to be considered when CWSI is used as a proxy for the stomatal conductance under different water stress conditions in the context of precision agriculture. When entire tree crowns are used, and when pixels are affected by background and soil, the CWSI values fall outside the expected theoretical range of variation. Under these conditions, the relationship CWSI vs. Gs is largely affected.

6. ACKNOWLEDGEMENTS

7. REFERENCES

[1]   S. B. Idso, R. D. Jackson, P. J. Pinter, R. J. Reginato, and J. L. Hatfield, "Normalizing the stress-degree-day parameter for environmental variability," *Agric. Meteorol.*, vol. 24, no. C, pp. 45–55, 1981.

[2]   R. D. Jackson, S. B. Idso, R. J. Reginato, and J. P. J. Pinter, "Canopy temperature as a crop water stress indicator," *Water Resour. Res.*, vol. 17, no. 4, pp. 1133–1138, 1981.

[3]   J. Berni, P. J. Zarco-Tejada, L. Suarez, and E. Fereres, "Thermal and Narrowband Multispectral Remote Sensing for Vegetation Monitoring From an Unmanned Aerial Vehicle," *IEEE Trans. Geosci. Remote Sens.*, vol. 47, no. 3, pp. 722–738, 2009.

[4]   S. B. Idso, R. J. Reginato, K. L. Clawson, and M. G. Anderson, "On the stability of non-water-stressed baselines," *Agric. For. Meteorol.*, vol. 32, no. 2, pp.

177–182, 1984.

[5] R. D. Jackson, R. J. Reginato, and S. B. Idso, "Wheat canopy temperature: A practical tool for evaluating water requirements," *Water Resour. Res.*, vol. 13, no. 3, pp. 651–656, 1977.

[6] G. Sepulcre-Cantó *et al.*, "Monitoring yield and fruit quality parameters in open-canopy tree crops under water stress. Implications for ASTER," *Remote Sens. Environ.*, vol. 107, no. 3, pp. 455–470, 2007.

[7] P. J. Zarco-Tejada, V. González-Dugo, and J. A. J. Berni, "Fluorescence, temperature and narrow-band indices acquired from a UAV platform for water stress detection using a micro-hyperspectral imager and a thermal camera," *Remote Sens. Environ.*, vol. 117, pp. 322–337, 2012.

[8] V. Gonzalez-Dugo, D. Goldhamer, P. J. Zarco-Tejada, and E. Fereres, "Improving the precision of irrigation in a pistachio farm using an unmanned airborne thermal system," *Irrig. Sci.*, vol. 33, no. 1, pp. 43–52, 2015.

[9] P. J. Zarco-Tejada, M. V. González-Dugo, and E. Fereres, "Seasonal stability of chlorophyll fluorescence quantified from airborne hyperspectral imagery as an indicator of net photosynthesis in the context of precision agriculture," *Remote Sens. Environ.*, vol. 179, pp. 89–103, 2016.

[10] V. Gonzalez-Dugo, P. Zarco-Tejada, J. A. J. Berni, L. Suárez, D. Goldhamer, and E. Fereres, "Almond tree canopy temperature reveals intra-crown variability that is water stress-dependent," *Agric. For. Meteorol.*, vol. 154–155, pp. 156–165, 2012.

[11] R Core Team, "R Core Team (2015). R: A language and environment for statistical computing.," *R Found. Stat. Comput. Vienna, Austria. URL http//www.R-project.org/.*, 2015.

[12] V. Gonzalez-Dugo, P. Hernandez, I. Solis, and P. J. Zarco-Tejada, "Using high-resolution hyperspectral and thermal airborne imagery to assess physiological condition in the context of wheat phenotyping," *Remote Sens.*, vol. 7, no. 10, pp. 13586–13605, 2015.